Journal of Nuclear Medicine, published on November 15, 2018 as doi:10.2967/jnumed.118.217745

First-in-human trial of ^{64}Cu-SARTATE PET imaging of patients with neuroendocrine tumours demonstrates high tumor uptake and retention, potentially allowing prospective dosimetry for peptide receptor radionuclide therapy

Running Title: CuSARTATE first in human in NET

Authors: Rodney J. Hicks[1,2], Price Jackson[1], Grace Kong[1], Robert E. Ware[1], Michael S. Hofman[1,2], David A. Pattison[1], Timothy A. Akhurst[1], Elizabeth Drummond[1], Peter Roselt[1], Jason Callahan[1], Roger Price[3], Charmaine M. Jeffery[3], Emily Hong[1], Wayne Noonan[4], Alan Herschtal[5], Lauren J. Hicks[6], Amos Hedt[7], Matthew Harris[7], Brett M. Paterson[8], Paul S. Donnelly[9].

[1] Cancer Imaging, the Peter MacCallum Cancer Centre, Melbourne, VIC, Australia
[2] The Sir Peter MacCallum Department of Oncology, the University of Melbourne, Parkville, VIC, Australia
[3] Medical Technology & Physics, Sir Charles Gairdner Hospital, Nedlands, WA, Australia
[4] Liverpool Hospital, Liverpool, NSW, Australia
[5] Biostatistics and Clinical Trials, the Peter MacCallum Cancer Centre
[6] The Mercy Hospital for Women, Heidelberg, VIC, Australia
[7] Clarity Pharmaceuticals Ltd, Eveleigh, NSW, Australia
[8] School of Chemistry, Monash University, VIC, Australia
[9] School of Chemistry and Bio21 Molecular Science and Biotechnology Institute, The University of Melbourne, Parkville, VIC, Australia

Acknowledgement of research support: This study was funded by Clarity Pharmaceuticals. Professor Hicks is the recipient of a National Health and Medical Research Council Practitioner Fellowship (APP1108050), which supported this work.

Disclaimers: We wish to confirm the following conflicts of interest associated with this publication. Amos Hedt and Matthew Harris are employed by Clarity Pharmaceuticals, the licensee of the intellectual property for SARTATE. Charmaine Jeffery has Clarity Pharmaceuticals share options. Paul S Donnelly and Brett M Paterson are inventors of, and hold intellectual property in, this area of research, which has been licensed from the University of Melbourne to Clarity Pharmaceuticals. Brett M Paterson and Paul S Donnelly possess share options in Clarity Pharmaceuticals. Paul S Donnelly serves on the Scientific Advisory Board of Clarity Pharmaceuticals. All other authors have no conflicts to declare directly related to this study. Unrelated to this project, Rodney J Hicks has share options in Telix Radiopharmaceuticals that are held on behalf of the Peter MacCallum Cancer Centre.

Corresponding author: Professor Rodney J Hicks, MD
Director, Molecular Imaging and Therapeutic Nuclear Medicine
The Peter MacCallum Cancer Centre, Cancer Imaging,
Level 5, 305 Grattan St Melbourne VIC 3000, Australia
Ph: +61-3-855-96618 Fax: +61-3-855-96619
Email: rod.hicks@petermac.org
Reprints are not available.

Word count (abstract and body text): 3,731

ABSTRACT

Imaging of somatostatin receptor (SSTR) expression is an established technique for staging of neuroendocrine neoplasia (NEN) and determining the suitability of patients for peptide receptor radionuclide therapy (PRRT). PET/ CT utilizing ^{68}Ga-labeled somatostatin analogues (SSAs) is superior to earlier agents, but the rapid physical decay of the radionuclide poses logistic and regulatory challenges. ^{64}Cu has attractive physical characteristics for imaging and provides a diagnostic partner for the therapeutic radionuclide ^{67}Cu. Based on promising pre-clinical studies, we have performed a first-time-in-human trial of ^{64}Cu-MeCOSar-octreotate (^{64}Cu-SARTATE) to assess its safety and ability to localise disease at early and late imaging time-points.

Methods: In a prospective trial, 10 patients with known NEN and positive ^{68}Ga-DOTA-octreotate (GaTate) PET/CT underwent serial PET/CT imaging at 30 min, 1, 4- and 24-hours following injection of ^{64}Cu-SARTATE. Adverse reactions were recorded, and laboratory testing was performed during infusion and at 1- and 7-days post-imaging. Images were analysed for lesion and normal organ uptake and clearance to assess lesion contrast and perform dosimetry estimates.

Results: ^{64}Cu-SARTATE was well tolerated during infusion and throughout the study, with three patients experiencing mild infusion-related events. High lesion uptake and retention were observed at all imaging time-points. There was progressive hepatic clearance over time, providing highest lesion to liver contrast at 24 hours. Image quality remained high at this time. Comparison of ^{64}Cu-SARTATE PET/CT obtained at 4 hours to GaTate PET/CT obtained at 1 hour indicated comparable or superior lesion detection in all patients, especially in the liver. As expected, highest early physiologic organ uptake was observed in the kidneys, liver and spleen.

Conclusion: ^{64}Cu-SARTATE is safe and has excellent imaging characteristics. High late-retention in tumour and clearance from the liver suggests suitability for diagnostic studies as well as for prospective dosimetry for ^{67}Cu-SARTATE PRRT, while the half-life of ^{64}Cu would also facilitate GMP production and distribution to sites without access to ^{68}Ga.

INTRODUCTION

Positron emission tomography/computed tomography (PET/CT) using ^{68}Ga-DOTA-Octreotate (GaTate), marketed commercially as NETSPOT® (Advanced Accelerator Applications, Saint-Genis-Pouilly, France) or other ^{68}Ga-labeled somatostatin analogues (SSAs), is becoming the gold standard for neuroendocrine neoplasia (NEN) diagnosis and staging (*1*). It is particularly important in determining the suitability of patients for peptide receptor radionuclide therapy (PRRT) (*2,3*). By virtue of its higher sensitivity for NEN than conventional imaging techniques, including ^{111}In-pentetreotide (Octreoscan™ , Mallinckrodt Pharmaceuticals, Dublin, Ireland) SPECT/CT, GaTate PET/CT has been shown to have a significant impact on patient management decisions (*4*). The efficacy and safety of PRRT depends on delivering the highest possible dose to the tumour deposits while sparing organs, particularly the kidneys, from radiation toxicity (*5-7*). While quantitative SPECT/CT techniques can provide verification of radiation dose delivered from each cycle of PRRT (*8*), ideally, dose estimation should be performed prior to therapeutic administration. Accurate prospective dosimetry would allow prescription of an administered activity that maximizes therapeutic efficacy within the tolerance of normal tissues. In the absence of such information, most facilities providing PRRT administer a standardized activity of 7-8 GBq of ^{177}Lu-labelled SSA or 2-4 GBq of ^{90}Y-labelled SSA. This strategy has generally been successful in providing moderate response rates with low toxicity as well as median progression-free and overall survival durations that have been encouraging in both single centre studies (*9*), as well as in the only randomised control trial performed to date, the NETTER-1 trial of ^{177}Lu-DOTA-octreotate (LuTate) versus dose-escalated SSA therapy (*10*). However, we believe that the therapeutic index may be further improved by an individualized rather than an empirical approach (*11*). Because of the so-called “sink effect”, changes in the burden of disease and tumour-avidity as treatment progresses can lead to marked variability in radiation delivery to both lesions and normal organs (*12*). The quantitative capability of PET/CT provides the

opportunity to assess uptake and retention of radioactive peptides in tumour and normal tissues and, thereby, to provide truly individualized prospective dosimetry. This was first demonstrated using ^{86}Y-SSA PET prior to ^{90}Y-SSA PRRT (*13*). While ^{68}Ga has been widely used as the diagnostic pair of ^{177}Lu, it has a half-life of only 68 minutes, which is insufficiently long to model the retention and clearance kinetics required for accurate dosimetry estimation in individual patients. This is particularly the case for organs with significant clearance over time, which include the kidneys and liver. Of longer-lived positron-emitting radioisotopes, the physical half-life of ^{64}Cu (12.7 hours) provides an opportunity to assess the clearance kinetics out to, and potentially beyond, 24 hours after tracer administration. This could also provide a diagnostic pair to both assess suitability of patients for ^{67}Cu PRRT and also enable predictive dosimetry. ^{67}Cu is a beta-emitting radionuclide with favourable physical characteristics for therapeutic application (*14*).

Our group has recently reported the synthesis and pre-clinical evaluation of ^{64}Cu-MeCOSar-Tyr3-octreotate (^{64}Cu-SARTATE) (*15*) based on a cage amine ligand called sarcophagine (Sar). An advantage of the MeCOSar, when compared to DOTA, is that copper (II) sarcophagine complexes are more stable than copper (II) DOTA complexes. In a murine xenograft model, the uptake of ^{64}Cu-SARTATE in SSTR-expressing tumours after 2 hours was high at 63.0 ± 15.0 %ID/g and remained high after 24 hours at 105 ± 27.1 %ID/g. This high retention at late time-points suggests superior potential for personalized PRRT dosimetry planning and therapeutic application. Accordingly, we have performed a single centre open-label, phase-0-1 investigation of ^{64}Cu-SARTATE in patients with World Health Organisation grade 1 or 2 NEN. Our hypotheses were that ^{64}Cu-SARTATE can be safely administered to humans and will facilitate identification of SSTR-expressing tissues using PET/CT scanning, with absorbed radiation doses that are appropriate for clinical use but with sufficient late retention to enable prospective radiation dosimetry.

MATERIALS AND METHODS

The trial protocol was approved by our institutional ethics committee as a first-time-in-human study and was registered with the Therapeutic Goods Administration as an Australian Clinical Trial Notification (ACTN 2015/0320). All patients provided written informed consent. The study was pragmatically designed to include up to 10 participants. Interim safety analyses were planned after 1, 2 and 5 study subjects had completed all required investigations. The trial flow-chart is displayed in Figure 1.

The primary objectives of this study were to estimate:

1. The rate of occurrence of adverse clinical, biochemical or haematological events following ^{64}Cu-SARTATE administration.
2. The percentage of injected dose and standardized uptake values of ^{64}Cu-SARTATE found in organs of interest at early and late time-points following administration of the investigational product.
3. Absorbed organ doses expressed as μGy/MBq of administered ^{64}Cu-SARTATE, and whole-body dose expressed as mSv/200MBq of administered activity.

The secondary objectives of this study were to determine whether ^{64}Cu-SARTATE PET/CT scans at 1, 4 hour and 24 hours demonstrate known sites of malignancy with tumour to background ratios that are equivalent to, or greater than, those achieved using routine clinical acquisition of GaTate at 1 hour, thereby enabling same-day diagnostic evaluation, and if there is ongoing lesion retention of tracer on the day after administration, to support its use for prospective radiation dosimetry calculations as an aid in the development of ^{67}Cu-SARTATE as a therapeutic agent. Reporting clinician preference for image quality was also assessed.

Eligibility criteria were as follows:

1. Signed informed consent.

2. Age ≥ 18 years.
3. Life expectancy ≥ 8 weeks.
4. Biopsy-proven World Health Organisation G1 or G2 (Ki-67 index 0-2% and 3-20%, respectively) NEN.
5. At least one site of active somatostatin receptor positive malignancy, as demonstrated on ^{68}GaTate PET/CT scan performed as part of routine clinical care.
6. Creatinine clearance > 60ml/min as estimated by the Cockcroft-Gault formula (using actual body weight).
7. Eastern Cooperative Oncology Group (ECOG) performance of 0-2.

The exclusion criteria were:

1. Pregnant or breastfeeding females.
2. Known sensitivity or allergy to SSAs.
3. Interventional treatment received for NEN in the interval between ^{68}GaTate PET/CT & ^{64}Cu-SARTATE PET/CT scan.
4. Treatment with long-acting somatostatin analogues within 28 days prior to test agent administration.
5. Treatment with short-acting somatostatin analogues within 24 hours prior to test agent administration.
6. QTc interval > 0.44 seconds as measured by screening ECG.
7. Any serious medical condition that the investigator felt may interfere with the procedures or evaluations of the study.
8. Patients unwilling or unable to comply with protocol or with a history of non-compliance or inability to grant informed consent.

Safety Analysis

Safety evaluations were performed 1 day and 1 week following tracer administration. These included physical examination, full blood examination (FBE), urea and electrolytes (U&E), liver function tests (LFT) and electrocardiography (ECG). Patient-reported adverse events were recorded

during administration of the radiotracer and after each scan and reported using the Common Terminology Criteria for Adverse Events v4.0 as published by the National Cancer Institute (Bethesda, MD, USA).

Positron Emission Tomography and Computed Tomography (PET/CT)

The PET/CT scans were acquired on a Discovery 690 scanner (GE Medical Systems, Waukesha, WI, USA), which has time-of-flight acquisition and a 64-slice CT scanner. CT scans were performed from the vertex to the lower thighs for the purposes of attenuation correction, localization of lesions and estimation of tumour volumes. These findings were correlated with recent contrast-enhanced CT when available. A low-dose, non-contrast technique was used (140 kVp, 40-200 mAs, GE smart mA), with a final reconstructed slice thickness of 3.27mm. Our standard GaTate PET/CT acquisition protocol was used. This involves a weight-based, intravenous administration of 150-300 MBq of radiopeptide with acquisition of 6-8 bed positions (3 minutes per bed position). PET scans were reconstructed using the ordered subset estimation method (OSEM) with 2 iterations and 20 subsets with a 3.25mm filter in a 128 x 128 matrix over a 55mm reconstructed transaxial FOV.

^{64}Cu-SARTATE was prepared using a modified version of a previously described method (*15*). Briefly, ^{64}Cu(II) (500-800 MBq, 0.02 M HCl) was added to SARTATE (20μg) in a solution of 4% ethanol in 0.1M ammonium acetate and 1mg/mL gentisic acid, sodium salt (5mL). The reaction mixture was incubated for 30 minutes at room temperature, then passed through a Strata™-X (Phenomenex, Inc.) cartridge (30 mg). Cartridge retained ^{64}Cu-SARTATE was rinsed with saline for injection before elution with ethanol into a vial containing saline for injection. The contents of this vial were filtered through a 0.22uM filter. ^{64}Cu-SARTATE was recovered in 60–80% radiochemical yield with >95% radiochemical purity. Average peptide mass administered was 6.4+/- 4.7 μg (Range 3.6 to 19.5). After intravenous administration of approximately 200 MBq of ^{64}Cu-SARTATE (Mean 192+/- 24 MBq and Range 125-209 MBq), PET scans

were acquired over the same axial extent with 3D acquisition of 8 bed positions (1.5 minutes per bed position for T30 scan and T60 scans, 2.0 minutes for T240 scans and 3 minutes for T24 hour scan). PET scans were reconstructed with 2 iterations, 18 subsets, and 7mm Gaussian smoothing kernel to mitigate image noise. All scans were performed at mean of 14 +/- 9 days (Range 6-27 d) of the GaTate PET/CT that determined eligibility for the study.

Analysis of ^{64}Cu-SARTATE Scans

Qualitative analysis of each subject's PET/CT scans was performed independently by 2 qualified nuclear medicine physicians blinded to clinical details of the patient. The GaTate and ^{64}Cu-SARTATE scans obtained at approximately 1 hour were presented side-by-side in a de-identified manner with the physician indicating image quality of each scan on a 5-point scale. They then indicated if any suspicious lesions were identified on one scan but not seen on the other. The number and location of such discordant lesions were recorded. Following this direct comparison of each scan type at the 1-hour time-point, the series of four individual ^{64}Cu-SARTATE image sets acquired from 30 minutes to 24 hours post-injection were displayed in a random order against each other and the GaTate images. The physician was asked to score image quality for each time point and to indicate whether any lesions were apparent on one scan but not the other.

Standardized uptake value (SUV) estimation was performed for up to 5 reference lesions (with no more than 3 per organ) on GaTate obtained at 1-hour post-injection using volume-of-interest software (MIM Encore™, MIM Software Inc., Cleveland, OH). If able to be identified, the same lesions were analysed on the ^{64}Cu-SARTATE scans at 1, 4 and 24 hours. Further, SUVmean estimations for normal liver, lungs, spleen, kidneys, bone marrow, thyroid, and pituitary gland were also obtained for ^{64}Cu-SARTATE at 1, 4 and 24 hours. Lesion-to-liver ratios were calculated for reference deposits at 1, 4 and 24 hours to determine the

optimal time for detection of hepatic lesions, which are common amongst patients with metastatic NEN (*16*).

For radiation cross-dose analysis, source organs considered were: adrenals, brain, upper and lower large intestinal contents, small intestine contents, stomach contents, heart contents, kidneys, liver, lungs, muscle, pancreas, red marrow, spleen, thyroid, urinary bladder contents, and the remainder of the body. Organs were contoured on the 30 minute PET/CT series and each subsequent time-point was fused by rigid and deformable image registration (*17*). For each contoured region, mean activity concentration was recorded, and total region activity determined based on standard MIRD adult source organ volumes. Three-phase time-activity curves were generated through automated routine (*18*) and integrated cumulated activity values (MBq*h/MBq) were converted to organ self- and cross-doses using OLINDA dose factors (s-values) (*19*). Mean organ doses, effective dose contribution, and total effective dose are reported based on ICRP-89 tissue weighting factors.

Statistical Analysis

All statistical analyses were performed in the R statistical software package version 3.4.2 using standard and validated statistical procedures. All statistical analysis results and their interpretation were independently reviewed by a qualified statistician. The mean, median and range of the % of injected tracer dose found in each organ of interest (liver, lungs, spleen, kidneys, bone marrow, thyroid, pituitary gland) across the 10 patients at each of the above time points are reported using standard reporting of descriptive baseline statistics including means, standard deviations, medians and ranges for continuous valued variables, and cell counts and percentages for categorical valued variables. Statistical methods consisted of production of Bland-Altman plots and Wilcoxon tests for paired data, carried out using the base package of the R language for statistical computing and commonly used add-on packages (gdata, Hmisc, plyr,

R2wd, and utils). P values of <0.05 on paired analyses were considered significant.

RESULTS

A total of 10 patients were recruited between June and October 2015. Clinical characteristics of these patients are included in Table 1.

Safety of ^{64}Cu-SARTATE

No grade 3 or 4 adverse events were reported. A single grade 2 event was recorded (transient wheezing). However, this was considered unrelated to treatment. Five grade 1 events were recorded; 2 were considered unrelated to the investigational agent (nausea and petechial rash); 2 were considered possibly related (flushing and leukopenia); and 1 (lymphopenia) was considered to be probably related to the investigational agent. Except for the 2 haematologic reactions, the adverse events were of short duration (< 7 days). The patient with lymphopenia (pt. 9) had previously received peptide receptor radionuclide therapy and had lymphocyte counts persistently in the lower end of the normal range since treatment. These dipped to 0.95 $x10^9$/L (N 1.00-4.00 $x10^9$/L) at 1 week after the scan before returning to the low normal range within 4 weeks. The patient with leukopenia (pt. 6) had a normal baseline white cell count that dropped to 3.9 $x10^9$/L (N >4.00 $x10^9$/L) at six weeks following the scan before returning to the normal range by follow-up at 3 months.

Percentage of Injected Dose (%ID) and SUV in Reference Organs and Tissues

The %ID in reference tissues and organs are detailed for each imaging time-point in Table 2. As expected, there was relatively rapid clearance of blood pool activity, slower clearance of renal activity and intermediate clearance of hepatic activity. High retention was seen in tumour and organs with high SSTR-expression, including the pituitary and spleen.

Comparison of Same-Day GaTate and ^{64}Cu-SARTATE Images

Comparison of the baseline ^{68}GaTate and serial ^{64}Cu-SARTATE images in all patients is displayed in Figure 2 using an upper threshold SUV of 20. The quality of images obtained at one hour with ^{64}Cu-SARTATE was judged to be comparable with those obtained using GaTate in 9/10 patients. One patient had superior definition of small liver lesions on GaTate and was judged as being diagnostically superior by 2 of 3 blinded readers. However, the 4-hour image in this patient was felt to be comparable to, and the 24-hour ^{64}Cu-SARTATE was judged by all readers to be superior to, the GaTate PET/CT obtained at 1 hour. The SUVmax of the most intense lesion (Max lesion) and mean of up to 5 reference lesions (Mean patient SUVmax) selected on the basis of baseline GaTate (Median 4, mean 3.3 and range 1-5 lesions) for each individual patient, were significantly lower for GaTate than for ^{64}Cu-SARTATE at both 1 and 4 hours (Table 3). While the SUVmax of lesions did not change significantly on ^{64}Cu-SARTATE between 4 and 24 hours, the progressive increase in lesion to liver ratio suggests that delayed imaging would provide optimal lesion detection (Table 4). Figure 3 provides an example of improved lesion detection on late imaging.

Delayed Image Quality

Image quality remained high at 24 hours following administration of ^{64}Cu-SARTATE (Figure 2). The delayed images demonstrated clearance of activity from the liver relative to tumour resulting in qualitatively improved image quality. This reflected primarily washout of liver activity as the median SUV_{max} of lesions at 24 hours was not significantly different to that at 4 hours (34.8 versus 33.3, P= 0.16).

Radiation Dosimetry

Dose estimates for major organs are presented in Table 5. Mean effective dose was 8.7±1.6 mSv per administration (mean injected activity 192MBq) or 0.0454mSv/MBq. Accordingly, an administered activity of 200MBq would give an

effective whole-body dose of approximately 9mSv plus that related to the CT component of the study.

DISCUSSION

There is increasing evidence that changing either the radionuclide or the chelating agent can alter affinity of SSAs for somatostatin receptors (*20*). Accordingly, the performance of novel radiopharmaceuticals cannot be reliably predicted by the receptor-binding affinity of the peptide (*21*). Additionally, when a long-lived radioisotope is used, retention of activity at sites of disease is important both for diagnostic and therapeutic purposes. The radionuclides ^{64}Cu and ^{67}Cu are an attractive theranostic pair. The main advantages of ^{64}Cu as a diagnostic agent are its favourable positron energy, cyclotron production and a half-life that enables both distribution to sites without on-site radiochemistry and delayed imaging after administration to patients (*22*). Imaging of tissue clearance kinetics will aid prospective dosimetry calculations for its therapeutic pair, ^{67}Cu, which also has favourable physical decay characteristics (*14*). These include a beta energy that is very similar to ^{177}Lu (580 keV versus 497 keV) but with a significantly shorter half-life (2.58 days versus 6.71 days), providing a higher dose-rate.

The first study to use ^{64}Cu to image NET was completed by Anderson *et al.* in 2001 (*23*). Eight subjects with a history of NET were imaged by conventional scintigraphy with ^{111}In-pentetreotide, followed by PET imaging with ^{64}Cu-TETA-octreotide. PET images were collected at times ranging from 0 to 36 hours after injection. Although a formal analysis of temporal changes in tracer uptake in tumour deposits was not performed, the authors noted that lesions were more clearly visualized on the early images than on the delayed images and that the best imaging time appeared to be approximately 4 – 6 h after tracer injection. A subsequent study completed by Pfeifer *et al.* (*24*), investigated the biodistribution and image quality of ^{64}Cu-DOTA-octreotate (^{64}Cu-DOTATATE) in 14 subjects with histologically confirmed NET, again with comparison to ^{111}In-

pentetreotide. PET/CT scans were acquired at 1 hour, 3 hours and 24 hours after administration. Compared with conventional scintigraphy, ^{64}Cu-DOTATATE PET/CT identified additional lesions in 6 of 14 (43%) patients. However, the images presented in this paper also suggest poor visualization of lesions at 24-hours. A more recent paper from the same group compared ^{64}Cu-DOTATATE PET/CT to ^{111}In-pentetreotide SPECT/CT in 111 patients but imaged patients with the PET tracer only at 1 hour after tracer administration (*25*). While this emulates the time at which ^{68}Ga tracers are typically imaged, it doesn't leverage the potential advantages of the longer half-life of ^{64}Cu. To our knowledge, no direct comparison of ^{64}Cu-DOTATATE and ^{68}GaTate in humans has been reported.

As well as assessing its safety, this first-time in human study was designed to assess whether the high binding-affinity of the MeCOSar chelating agent for ^{64}Cu observed in murine models (*15*), is reproduced in humans. Supporting the pre-clinical promise of this agent, there was high retention in tumour deposits and substantial hepatic clearance leading to a significant increase in lesion contrast in the liver, as well as excellent ongoing visualisation of extra-hepatic disease. Image quality and SUV analysis suggests that, for the patient convenience of same-day imaging, acquisition at 4 hours would be optimal, although earlier imaging is feasible, being comparable with GaTate PET/CT in the majority (9/10) of patients. Although less convenient for patients, delayed imaging at 24 hours is also feasible with particularly high lesion-to-liver contrast at this time, potentially improving sensitivity of detection of disease in this organ, which is a major site of metastases in NEN (*26*).

Since all patients were selected on the basis of a positive ^{68}GaTate scan, the utility of ^{64}Cu-SARTATE in patients with low or absent tumour uptake on ^{68}GaTate PET/CT could not be assessed. Another potential limitation is that ^{68}GaTate PET/CT always preceded the ^{64}Cu-SARTATE study. However, reference lesions were all first defined on the ^{68}GaTate study and were the most

intense lesions on this scan. Accordingly, the likelihood of partial volume effects was low on the initial scan and given selection of G1-2 patients, the likelihood of significant growth through the partial volume count recovery curve accounting for increased lesion visualisation is low with a mean delay of only 14 days between the scans.

No significant adverse events were seen with ^{64}Cu-SARTATE administration. The transient minor reduction in lymphocyte and leukocyte counts in 2 patients did not appear to be related to radiation dose to either spleen or red marrow, which were similar to those in other patients. This may represent normal fluctuation in these counts given both had counts that were otherwise persistently in the lower end of the normal range, in one case probably related to prior radionuclide therapy. We don't consider that these findings are likely impact the suitability of this peptide as a therapeutic agent. The effective whole-body radiation dose was approximately 9mSv for a 200MBq (0.0454mSv/MBq) administered activity. This estimate is in keeping with the long physical half-life and per-decay energy emission of Cu-64 relative to other PET isotopes as well as previous dose reports for ^{64}Cu-DOTATATE by Pfeifer et al. (0.0315 mSv/MBq) (*24*). Organ doses were also comparable to the Pfeifer publication, although kidney and spleen doses were higher as indicated by the SUV data. These slight differences between dosimetry data may be related to the biological affinity of SARTATE vs DOTA-octreotate molecules for SSTR-2 and altered clearance from normal organs.

CONCLUSION

High uptake and retention of ^{64}Cu-SARTATE in tumors and accompanying clearance of activity from the liver provides high-contrast diagnostic images until at least 24 hours after injection, increasing the flexibility for timing of diagnostic imaging and the potential for multiple time-point dosimetry estimation prior to ^{67}Cu-SARTATE PRRT. The longer half-life of ^{64}Cu compared with ^{68}Ga also makes this agent suitable for commercial GMP production and distribution to

remote sites. This preliminary evaluation indicates that the agent is safe and has acceptable radiation dosimetry for human use as a diagnostic agent, with improved imaging characteristics at 4 hours compared to 1 hour.

ACKNOWLEDGEMENTS

The authors wish to thank the patients involved for their participation in the study and the Molecular Imaging Team and Neuroendocrine Tumour Service for their diligence in caring for their excellent work. Professor Hicks is supported by a National Health and Medical Research Council Practitioner Fellowship (APP1108050).

References

1. Deppen SA, Blume J, Bobbey AJ, et al. 68Ga-DOTATATE Compared with ^{111}In-DTPA-octreotide and conventional imaging for pulmonary and gastroenteropancreatic neuroendocrine tumors: a systematic review and meta-analysis. *J Nucl Med.* 2016;57:872-878.

2. Hicks RJ. Use of molecular targeted agents for the diagnosis, staging and therapy of neuroendocrine malignancy. *Cancer Imaging.* 2010;10 Spec no A:S83-91.

3. Kwekkeboom DJ, de Herder WW, van Eijck CH, et al. Peptide receptor radionuclide therapy in patients with gastroenteropancreatic neuroendocrine tumors. *Semin Nucl Med.* 2010;40:78-88.

4. Hofman MS, Hicks RJ. Changing paradigms with molecular imaging of neuroendocrine tumors. *Discov Med.* 2012;14:71-81.

5. Bodei L, Cremonesi M, Ferrari M, et al. Long-term evaluation of renal toxicity after peptide receptor radionuclide therapy with ^{90}Y-DOTATOC and ^{177}Lu-DOTATATE: the role of associated risk factors. *Eur J Nucl Med Mol Imaging.* 2008;35:1847-1856.

6. Kashyap R, Jackson P, Hofman MS, et al. Rapid blood clearance and lack of long-term renal toxicity of ^{177}Lu-DOTATATE enables shortening of renoprotective amino acid infusion. *Eur J Nucl Med Mol Imaging.* 2013;40:1853-1860.

7. Sabet A, Ezziddin K, Pape UF, et al. Accurate assessment of long-term nephrotoxicity after peptide receptor radionuclide therapy with ^{177}Lu-octreotate. *Eur J Nucl Med Mol Imaging.* 2014;41:505-510.

8. Beauregard J-M, Hofman MS, Pereira JM, Eu P, Hicks RJ. Quantitative ^{177}Lu SPECT (QSPECT) imaging using a commercially available SPECT/CT system. *Cancer Imaging.* 2011;11:56-66.

9. Hicks RJ, Kwekkeboom DJ, Krenning E, et al. ENETS consensus guidelines for the standards of care in neuroendocrine neoplasia: peptide receptor radionuclide therapy with radiolabeled somatostatin analogues. *Neuroendocrinology.* 2017;105:295-309.

10. Strosberg J, El-Haddad G, Wolin E, et al. Phase 3 Trial of 177Lu-Dotatate for Midgut Neuroendocrine Tumors. *N Engl J Med.* 2017;376:125-135.

11. Hofman MS, Hicks RJ. Peptide receptor radionuclide therapy for neuroendocrine tumours: standardized and randomized, or personalized? *Eur J Nucl Med Mol Imaging.* 2014;41:211-213.

12. Beauregard JM, Hofman MS, Kong G, Hicks RJ. The tumour sink effect on the biodistribution of 68Ga-DOTA-octreotate: implications for peptide receptor radionuclide therapy. *Eur J Nucl Med Mol Imaging.* 2012;39:50-56.

13. Pauwels S, Barone R, Walrand S, et al. Practical dosimetry of peptide receptor radionuclide therapy with (90)Y-labeled somatostatin analogs. *J Nucl Med.* 2005;46 (Suppl 1):92S-98S.

14. Novak-Hofer I, Schubiger PA. Copper-67 as a therapeutic nuclide for radioimmunotherapy. *Eur J Nucl Med Mol Imaging.* 2002;29:821-830.

15. Paterson BM, Roselt P, Denoyer D, et al. PET imaging of tumours with a 64Cu labeled macrobicyclic cage amine ligand tethered to Tyr3-octreotate. *Dalton Trans.* 2014;43:1386-1396.

16. Frilling A, Clift AK. Therapeutic strategies for neuroendocrine liver metastases. *Cancer.* 2015;121:1172-1186.

17. Klein S, Staring M, Murphy K, Viergever MA, Pluim JP. Elastix: a toolbox for intensity-based medical image registration. *IEEE Trans Med Imaging.* 2010;29:196-205.

18. Jackson PA, Beauregard J-M, Hofman MS, Kron T, Hogg A, Hicks RJ. An automated voxelized dosimetry tool for radionuclide therapy based on serial quantitative SPECT/CT imaging. *Medical Physics.* 2013; 40:112503.

19. Stabin MG, Sparks RB, Crowe E. OLINDA/EXM: the second-generation personal computer software for internal dose assessment in nuclear medicine. *J Nucl Med.* 2005;46:1023-1027.

20. Fani M, Del Pozzo L, Abiraj K, et al. PET of somatostatin receptor-positive tumors using ^{64}Cu- and ^{68}Ga-somatostatin antagonists: the chelate makes the difference. *J Nucl Med.* 2011;52:1110-1118.

21. Hicks RJ. Citius, Altius, Fortius - An olympian dream for theranostics. *J Nucl Med.* 2017;58:194-195.

22. Williams HA, Robinson S, Julyan P, Zweit J, Hastings D. A comparison of PET imaging characteristics of various copper radioisotopes. *Eur J Nucl Med Mol Imaging.* 2005;32:1473-1480.

23. Anderson CJ, Dehdashti F, Cutler PD, et al. 64Cu-TETA-octreotide as a PET imaging agent for patients with neuroendocrine tumors. *J Nucl Med.* 2001;42:213-221.

24 Pfeifer A, Knigge U, Mortensen J, et al. Clinical PET of neuroendocrine tumors using 64Cu-DOTATATE: first-in-humans study. *J Nucl Med.* 2012;53:1207-1215.

25. Pfeifer A, Knigge U, Binderup T, et al. 64Cu-DOTATATE PET for Neuroendocrine Tumors: A Prospective Head-to-Head Comparison with 111In-DTPA-Octreotide in 112 Patients. *J Nucl Med.* 2015;56:847-854.

26. Frilling A, Modlin IM, Kidd M, et al. Recommendations for management of patients with neuroendocrine liver metastases. *Lancet Oncol.* 2014;15:e8-21.

Figure 1. Study Flow Chart

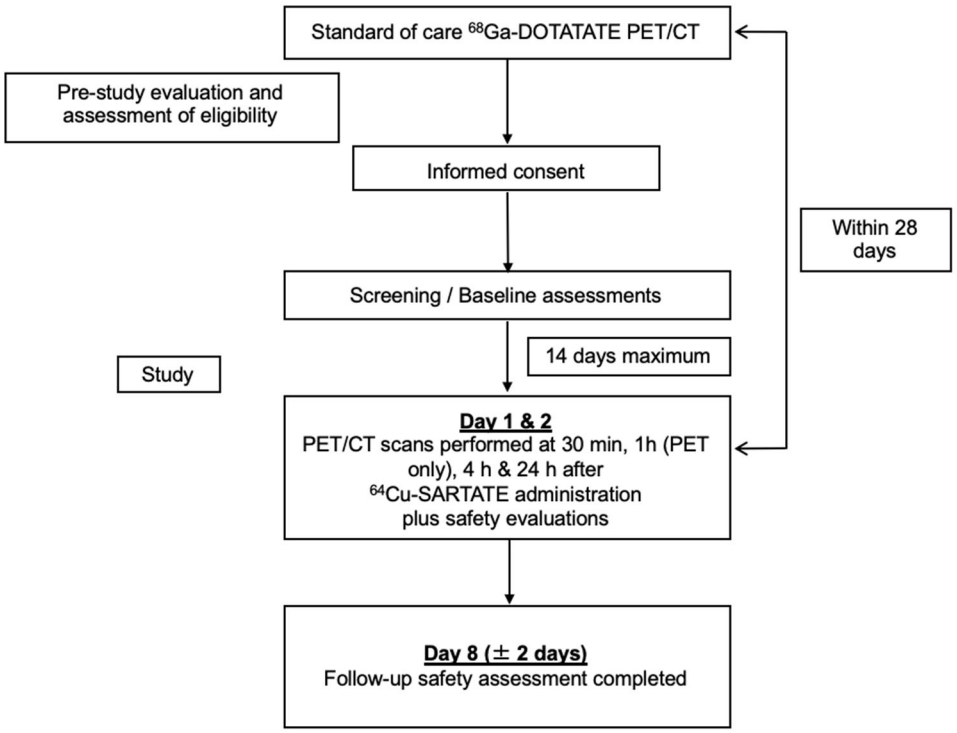

Figure 2. Comparison of Tracers

Maximum intensity projection (MIP) images obtained at 1 h for ^{68}Ga-DOTA-octreotate (GaTate) are compared with corresponding maximum intensity projection images acquired at 30 min, and at 1, 4 and 24 h after administration of ^{64}Cu-MeCOSAR-octreotate (CuSARTATE). Although CuSARTATE images were deemed comparable at 1 hour in 9/10 patients (pt. 6 was the exception), all were considered equivalent or superior to ^{68}GaTate at both 4 and 24 h.

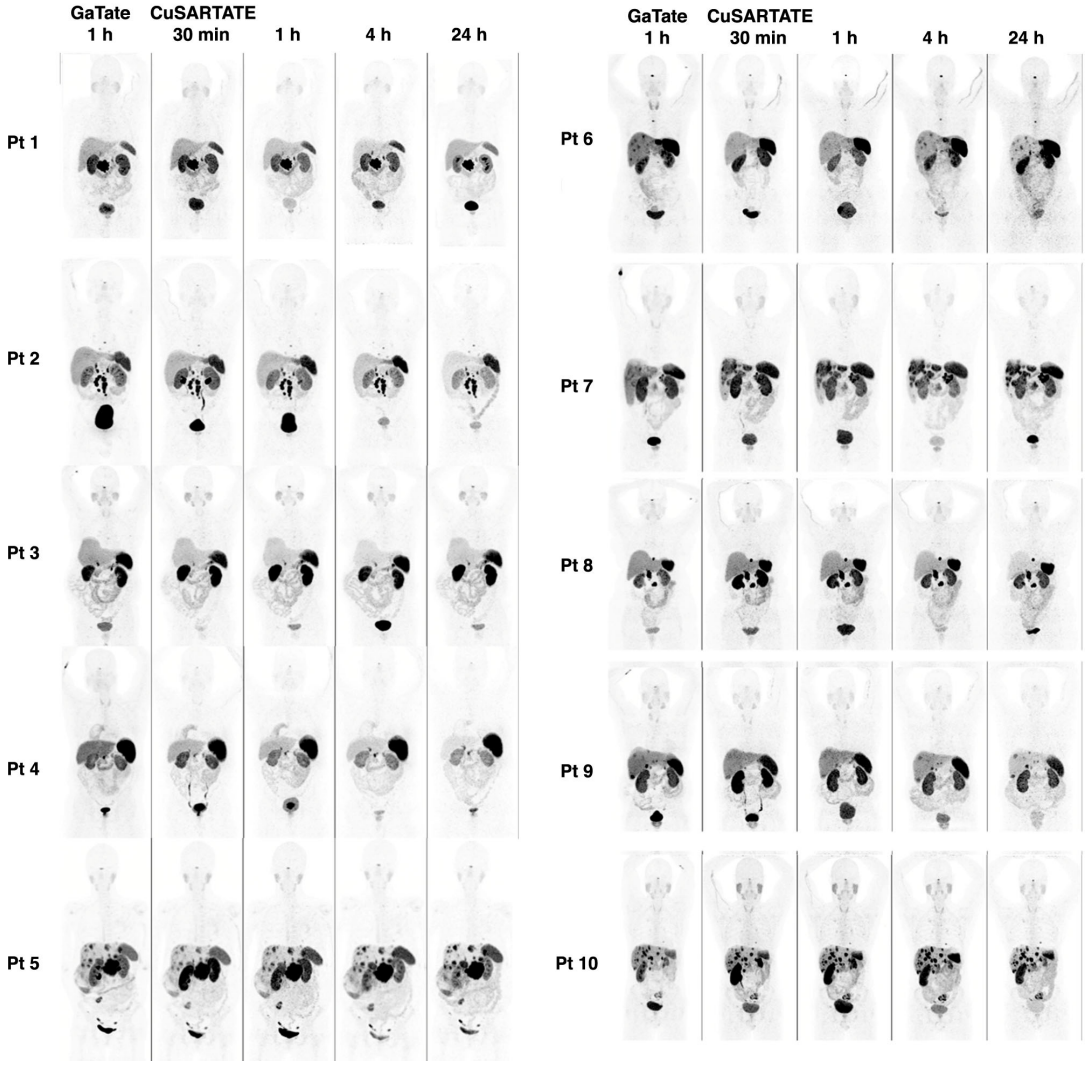

Figure 3. Superior lesion detection at 4-Hours

High lesion contrast on ^{64}Cu-MeCOSAR-octreotate images obtained at 4-hours provided better definition of regional nodal disease than in ^{68}Ga-DOTA-octreotate PET/CT obtained at 1-hour post-administration in this patient with a large pancreatic primary but slightly greater small bowel activity indicating some hepatobiliary excretion.

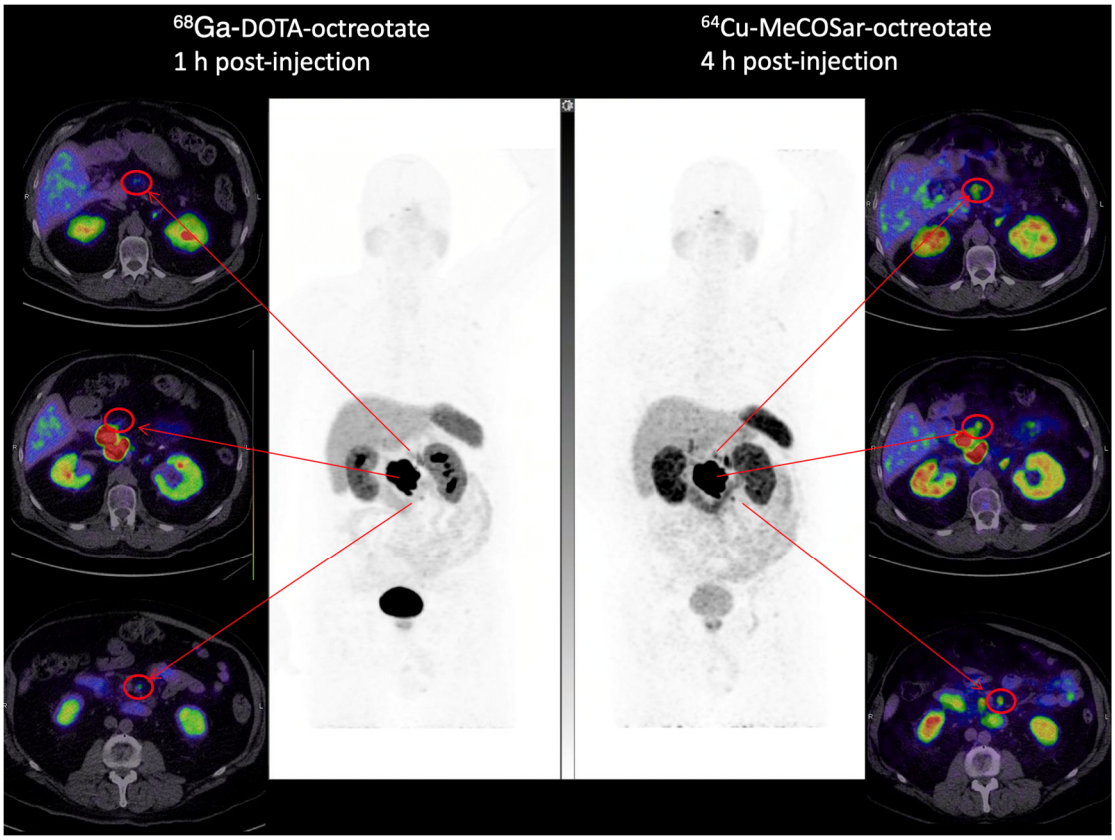

Table 1. Baseline Characteristics

Variable	Statistic / Level	Count / Value
Sex	F	4
	M	6
Age	Mean (SD)	63.2 (10)
	Median [range]	62 [46 - 78]
	Interquartile range	57.2 - 71.5
Baseline ECOG	0	6 (60%)
	1	4 (40%)
Baseline EGFR	≤70	3 (30%)
	>70	7 (70%)
Weight (kg)	Mean (SD)	87.7 (16)
	Median [range]	90.5 [60 - 112]
	Interquartile range	74.6 - 98
Height (cm)	Mean (SD)	173.2 (7)
	Median [range]	173 [163 - 185]
	Interquartile range	168 - 176.5

Table 2. Mean and SD of %ID of ^{64}Cu-SARTATE for Normal Organs

Organ	30 Minutes	1 Hour	4 Hours	24 Hours
Adrenals	0.19 (0.13)	0.17 (0.12)	0.19 (0.14)	0.17 (0.16)
Brain	0.23 (0.06)	0.17 (0.10)	0.22 (0.06)	0.16 (0.06)
Lower large intestine	0.42 (0.18)	0.44 (0.21)	0.47 (0.19)	0.69 (0.37)
Small intestine	4.40 (1.38)	4.32 (0.99)	3.78 (1.37)	2.90 (0.83)
Stomach	1.69 (1.26)	1.73 (1.22)	0.68 (0.87)	0.82 (0.61)
Upper large intestine	1.60 (1.59)	1.77 (1.65)	1.44 (1.19)	1.34 (0.59)
Heart	0.76 (0.37)	0.66 (0.31)	0.48 (0.30)	0.37 (0.19)
Kidneys	6.40 (1.59)	5.22 (1.51)	4.33 (0.91)	3.49 (0.68)
Liver	15.02 (2.06)	13.90 (2.30)	11.79 (3.12)	6.79 (2.87)
Lungs	0.99 (0.18)	0.90 (0.25)	0.66 (0.18)	0.46 (0.12)
Muscle	2.27 (0.48)	2.13 (0.44)	1.82 (0.51)	1.32 (0.36)
Pancreas	0.52 (0.25)	0.49 (0.31)	0.50 (0.39)	0.41 (0.24)
Red marrow	7.15 (1.39)	6.28 (1.39)	5.62 (1.38)	4.44 (0.99)
Spleen	4.68 (1.90)	4.94 (1.96)	5.41 (2.07)	4.06 (1.90)
Thyroid	0.05 (0.02)	0.04 (0.02)	0.04 (0.02)	0.04 (0.03)
Urinary bladder	5.27 (3.55)	5.72 (4.71)	2.13 (2.85)	1.49 (1.11)
Remainder of body	55.62 (11.63)	56.77 (12.44)	52.58 (14.02)	42.34 (13.45)

Table 3. Comparison of Lesion and Normal Organ Uptake and Retention for ^{68}Ga-DOTA-Octreotate (GaTate) and ^{64}Cu-MECOSAR-Octreotate (SARTATE)

Measure	Median GaTate at 1hr	Median SARTATE at 1 hr	Difference	95% CI	P-value
Max Lesion SUVmax	31.65	41.90	12.45	[5.1, 21.4]	0.010
Mean Patient SUVmax	23.61	33.32	10.35	[5.4, 15.3]	0.002
Liver SUVmean	7.10	7.45	0.30	[-0.2, 0.8]	0.24
Spleen SUVmean	20.40	28.25	9.05	[4.0, 14.9]	0.004
Kidney SUVmean	13.10	20.98	6.80	[5.4, 12.1]	0.002
Measure	**GaTate at 1hr**	**SARTATE at 4 hrs**	**Difference**	**95% CI**	**P-value**
Max Lesion SUVmax	31.65	50.50	17.10	[9.6, 36.3]	0.004
Mean Patient SUVmax	23.61	34.80	12.99	[6.3, 27.9]	0.004
Liver SUVmean	7.10	5.90	-1.05	[-2.2, 1.0]	0.19
Spleen SUVmean	20.40	35.55	17.50	[7.7,102.2]	0.020
Kidney SUVmean	13.10	18.05	4.86	[2.1,7.0]	0.004

Paired Wilcoxon tests in 10 patients

Table 4. Comparison of Lesion: Liver Ratios of ^{68}Ga-DOTA-Octreotate (GaTate) and ^{64}Cu-MECOSAR-Octreotate (SARTATE)

	Median		Median	Difference	95% CI	P-value
Mean GaTate: Liver Ratio (1 hr)	3.92	Mean Cu-SARTATE: Liver Ratio (1 hr)	5.45	1.35	[0.7, 2.2]	0.004
Mean GaTate: Liver Ratio (1 hr)	3.92	Mean Cu-SARTATE: Liver Ratio (4 hrs)	6.70	3.86	[1.5, 6.4]	0.002
Mean Cu-SARTATE: Liver Ratio 4hrs	6.70	Mean Cu-SARTATE: Liver Ratio (24 hrs)	16.69	6.75	[3.4, 10.3]	0.002

Paired Wilcoxon tests in 10 patients

Table 5. Table 5. Mean and SD range of absorbed organ doses (mGy/MBq) in comparison with previously reported ^{64}Cu-DOTATATE values from Pfeifer et al. (24)

Organ Dose Data (mSv/MBq)													
Patient	1	2	3	4	5	6	7	8	9	10	**Mean**	ST DEV	**Pfeifer et al 2012**
Adrenals	4.14E-01	1.81E-01	4.88E-02	1.96E-01	8.19E-02	5.67E-02	3.18E-02	2.36E-01	1.55E-01	2.91E-01	**1.69E-01**	1.22E-01	**1.37E-01**
Brain	1.53E-02	1.48E-02	2.19E-02	1.43E-02	9.45E-03	1.51E-02	1.39E-02	1.03E-02	1.20E-02	1.15E-02	**1.39E-02**	3.50E-03	**1.27E-02**
Breasts	1.38E-02	1.37E-02	2.07E-02	1.18E-02	8.86E-03	1.33E-02	1.18E-02	9.68E-03	1.09E-02	1.08E-02	**1.25E-02**	3.31E-03	**1.32E-02**
Gallbladder Wall	2.78E-02	2.79E-02	3.60E-02	2.33E-02	1.91E-02	2.43E-02	2.36E-02	1.94E-02	2.14E-02	2.14E-02	**2.44E-02**	5.06E-03	**3.96E-02**
LLI Wall	6.47E-02	3.24E-02	6.74E-02	7.06E-02	3.29E-02	4.44E-02	5.68E-02	2.90E-02	3.13E-02	5.35E-02	**4.83E-02**	1.63E-02	**4.32E-02**
Small Intestine	6.83E-02	5.53E-02	7.92E-02	8.36E-02	5.83E-02	8.59E-02	9.53E-02	6.16E-02	4.98E-02	6.88E-02	**7.06E-02**	1.49E-02	**6.55E-02**
Stomach Wall	6.92E-02	5.43E-02	3.85E-02	3.61E-02	4.13E-02	3.62E-02	2.58E-02	2.19E-02	4.87E-02	7.50E-02	**4.47E-02**	1.73E-02	**1.93E-02**
ULI Wall	5.33E-02	5.55E-02	7.02E-02	3.91E-02	4.39E-02	1.24E-01	7.74E-02	4.79E-02	5.37E-02	5.92E-02	**6.24E-02**	2.45E-02	**2.18E-02**
Heart Wall	2.66E-02	2.65E-02	3.69E-02	1.92E-02	1.62E-02	2.11E-02	2.33E-02	1.68E-02	2.98E-02	2.02E-02	**2.37E-02**	6.41E-03	**1.86E-02**
Kidneys	1.48E-01	1.88E-01	2.76E-01	2.20E-01	1.87E-01	2.42E-01	2.10E-01	1.82E-01	1.97E-01	1.73E-01	**2.02E-01**	3.66E-02	**1.39E-01**
Liver	1.20E-01	1.21E-01	1.14E-01	8.15E-02	8.14E-02	5.21E-02	7.88E-02	7.01E-02	7.56E-02	7.22E-02	**8.67E-02**	2.34E-02	**1.61E-01**
Lungs	2.75E-02	2.60E-02	2.89E-02	2.10E-02	1.71E-02	2.30E-02	2.39E-02	1.92E-02	2.03E-02	2.00E-02	**2.27E-02**	3.85E-03	**1.67E-02**
Muscle	1.68E-02	1.63E-02	2.43E-02	1.48E-02	1.10E-02	1.71E-02	1.50E-02	1.20E-02	1.37E-02	1.36E-02	**1.55E-02**	3.70E-03	**1.90E-02**
Ovaries	2.13E-02	1.96E-02	3.03E-02	2.07E-02	1.44E-02	2.44E-02	2.07E-02	1.53E-02	1.64E-02	1.79E-02	**2.01E-02**	4.68E-03	**1.92E-02**
Pancreas	9.40E-02	1.89E-01	7.24E-02	9.91E-02	4.48E-02	8.65E-02	6.95E-02	6.85E-02	1.05E-01	7.01E-02	**8.99E-02**	3.91E-02	**9.27E-02**
Red Marrow	4.87E-02	3.99E-02	6.23E-02	5.03E-02	3.23E-02	4.12E-02	4.34E-02	3.40E-02	4.47E-02	3.74E-02	**4.34E-02**	8.82E-03	**2.65E-02**
Osteogenic Cells	4.76E-02	4.26E-02	6.74E-02	4.57E-02	3.09E-02	4.36E-02	4.16E-02	3.31E-02	4.05E-02	3.69E-02	**4.30E-02**	1.01E-02	**3.35E-02**
Skin	1.29E-02	1.28E-02	1.98E-02	1.14E-02	8.36E-03	1.30E-02	1.12E-02	9.16E-03	1.02E-02	1.03E-02	**1.19E-02**	3.19E-03	**1.22E-02**
Spleen	2.47E-01	3.05E-01	3.33E-01	2.01E-01	2.64E-01	2.55E-01	3.97E-01	5.96E-01	6.20E-01	3.92E-01	**3.61E-01**	1.44E-01	**1.15E-01**
Testes	1.41E-02	1.38E-02	2.18E-02	1.30E-02	9.04E-03	1.55E-02	1.24E-02	9.78E-03	1.09E-02	1.13E-02	**1.31E-02**	3.64E-03	**1.36E-02**
Thymus	1.55E-02	1.53E-02	2.34E-02	1.33E-02	9.84E-03	1.49E-02	1.33E-02	1.07E-02	1.25E-02	1.21E-02	**1.41E-02**	3.77E-03	**1.49E-02**
Thyroid	5.24E-02	3.68E-02	8.06E-02	2.29E-02	1.98E-02	5.25E-02	4.32E-02	2.01E-02	3.72E-02	2.41E-02	**3.90E-02**	1.92E-02	**1.41E-02**
Urinary Bladder Wall	6.73E-02	6.03E-02	7.66E-02	1.27E-01	5.59E-02	2.16E-01	7.38E-02	4.91E-02	5.30E-02	6.61E-02	**8.46E-02**	5.13E-02	**3.70E-02**
Uterus	2.05E-02	1.93E-02	2.95E-02	2.08E-02	1.41E-02	2.56E-02	1.98E-02	1.49E-02	1.60E-02	1.73E-02	**1.98E-02**	4.81E-03	**1.89E-02**
Total Body	2.22E-02	2.17E-02	3.01E-02	1.97E-02	1.53E-02	2.10E-02	2.00E-02	1.68E-02	1.88E-02	1.80E-02	**2.04E-02**	4.06E-03	**2.50E-02**